Sensors & Actuators: A. Physical 349 (2023) 114083

Contents lists available at ScienceDirect

Sensors and Actuators: A. Physical

journal homepage: www.journals.elsevier.com/sensors-and-actuators-a-physical

Self-adaptive detachable pneumatic soft actuators using uniformly distributed temporary-bonding-fasteners for wearable applications

Haewon Jeong, Wei Dawid Wang *

Department of Mechanical Engineering, Hanyang University, Seoul 04763 the Republic of Korea

ARTICLE INFO

Keywords:
Soft wearable devices
Self-adaptive
Pneumatic soft actuators
Robotic gloves
Elbow assistance

ABSTRACT

Human skin, especially the skin above rotating joints, has numerous creases and folds, so it can stretch and shrink with the movement of the musculoskeletal system. When we bend our fingers or elbows where there are joints, not only the rotating of bone joints occurs but also obvious stretching of the covered skin. However, most designs of soft actuators for wearable rotation-assistance of joints do not take into account these bending and stretching coupled deformations but focus only on the bending deformations. This situation results in different degrees of buckling of soft actuators when bending with joints due to inconsistencies in deformation. This study demonstrates detachable pneumatic soft actuators (DPSAs) in a single design for wearable fabrics capable of generating self-adaptive bending and extending deformation when rotating the joint. The DPSA is that of a pneumatic soft linear actuator with temporary bonding fasteners uniformly distributed to one side of the soft actuator. The bonding fasteners enable the DPSA to easily attach to the stretchable fabrics and further to conformably fit the joints of the human body. The self-adaptability of DPSAs enables the fabrics to not only actively rotate the human joints but also passively accommodate large skin stretches, without buckling even at large offset distances. Moreover, DPSAs in a single design are capable of good interchangeability and reusability supported by temporary bonding fasteners. Applications for both robotic glove and elbow assistance are finally demonstrated by utilizing identical DPSAs.

1. Introduction

The market for wearable devices, especially the need for mobility assistance and rehabilitation, is growing rapidly due to aging and related diseases such as stroke [1–4]. These wearable devices are capable of providing external mechanical forces to assist the desired joint movement of users. Conventional exoskeletons serving as the external bones of the user are mainly composed of orthotic materials such as plastic and metal, which are compact but heavy and uncomfortable to wear. They also require the complex design of joints to customize for the individual user. In contrast, soft robotic wearables made of soft and smart materials to serve as external muscles are inherently compliant, flexible, and light in weight for better wearing comfort [5]. In addition, soft robotic wearables are capable of generating large deformations in various motions, such as bending, extending, and twisting. This flexibility creates numerous possibilities for applications [6–9].

Soft wearables for mobility assistance can be roughly divided into two types based on the relative positions of the wearables on the joints. One is fixed under the joint, and the other is attached to the outer surface of the joint. Several problems arise when soft wearables are located beneath the joint [10–14]. Due to their positions within the range of motion of the joints, they can hinder the movement, especially for bending motions such as making a fist or bending the elbow. Additionally, these soft wearables may interfere with perception by covering texture receptors on the fingertips and palms. On the other hand, attaching to the outer surface of the joint largely alleviates the problems above. This situation includes many actuation types, such as shape memory alloy (SMA)-based soft actuators [15–18] and pneumatic soft actuators [19–28]. Attaching the soft actuators to the outside surface of the bending mechanism introduces an offset distance between the neutral planes of the structures. The offset distance results in these soft actuators containing constraining layers that buckle and cannot bend due to the insufficient extending deformation being inconsistent with the stretch of the skin over joints [22–28], especially when large, non-uniform stretches occur (Fig. 1A and 1B). Therefore, the inconsistency between the actuator and the joints makes these soft bending actuators seldom used in applications with large offset distances, such as elbow joints.

* Corresponding author.
E-mail address: davidwang@hanyang.ac.kr (W.D. Wang).

https://doi.org/10.1016/j.sna.2022.114083
Received 29 June 2022; Received in revised form 18 November 2022; Accepted 7 December 2022
Available online 9 December 2022

Soft wearables with actuators segmented by the positions of multiple joints can have better coupling with body parts but cannot fundamentally solve the issues described above [29–31]. In addition, it is time-consuming to redesign and refabricate for different sizes of body parts. Therefore, there is a need to design self-adaptive wearables that are not affected by either the size or shape of human joints. Another need is for a single design for soft wearables capable of multiple applications to greatly reduce the cost. Further advantages of a single design, such as interchangeability and reusability, can be accomplished by introducing a dismountable design. A dismountable design can be achieved by using temporary bonding fasteners [32], popular in clothing to replace buttons or zippers, as a temporary bond to attach the soft actuators to the desired positions.

To address these issues, this study describes a design for self-adaptive wearables that are not affected by either the size or shape of human joints, and that enables multiple applications with a single design. The design was accomplished by conglutinating the small-sized temporary bonding fasteners evenly and discretely to one side of a single type of commonly used pneumatic soft linear actuator to form the detachable pneumatic soft actuators (DPSAs). The bonding fasteners enable the DPSAs to conformably attach to the surface of the human joints via stretchable fabrics, thus to produce self-adaptive bending-extending deformation for multiple wearable applications. After wearing the fabrics to the joints and attaching the DPSAs, the bonding interface between DPSAs and the fabrics automatically becomes the discontinued constraining layer. The DSPAs utilizing the discontinued constraining layer enable the fabrics to be capable of actively deforming to rotate the body joints and also passively adapt to the large stretches of the skin caused by joint motion. Moreover, the temporary bond allows identical DPSAs to be reutilized for different applications and to easily replace failed actuators. Finally, identical DPSAs were introduced to the design of both a robotic glove and elbow assistance.

2. Design and fabrication

Flexion of the human joints causes significant stretching of the skin. Experimental data show that the stretching of the skin is uneven and large, and the maximum stretching ratios at a finger joint and an elbow joint can reach about 40 % and 60 %. Therefore, it is needed to design soft wearable actuators that cannot only provide joint bending force but also accommodate the large and uneven stretches of the skin (Fig. 1A and B). The proposed basic actuator is a linear actuator in a serpentine configuration consisting of alternately arranged flat segments and curved segments. Flat segments serve as inflating chambers, and curved segments link these segments all together. Under pressurization, flat segments inflate and squeeze the adjacent inflated flat segments, which leads to a linearly extending deformation of the actuator (Fig. 1C). One side of the actuator is attached with uniformly distributed temporary

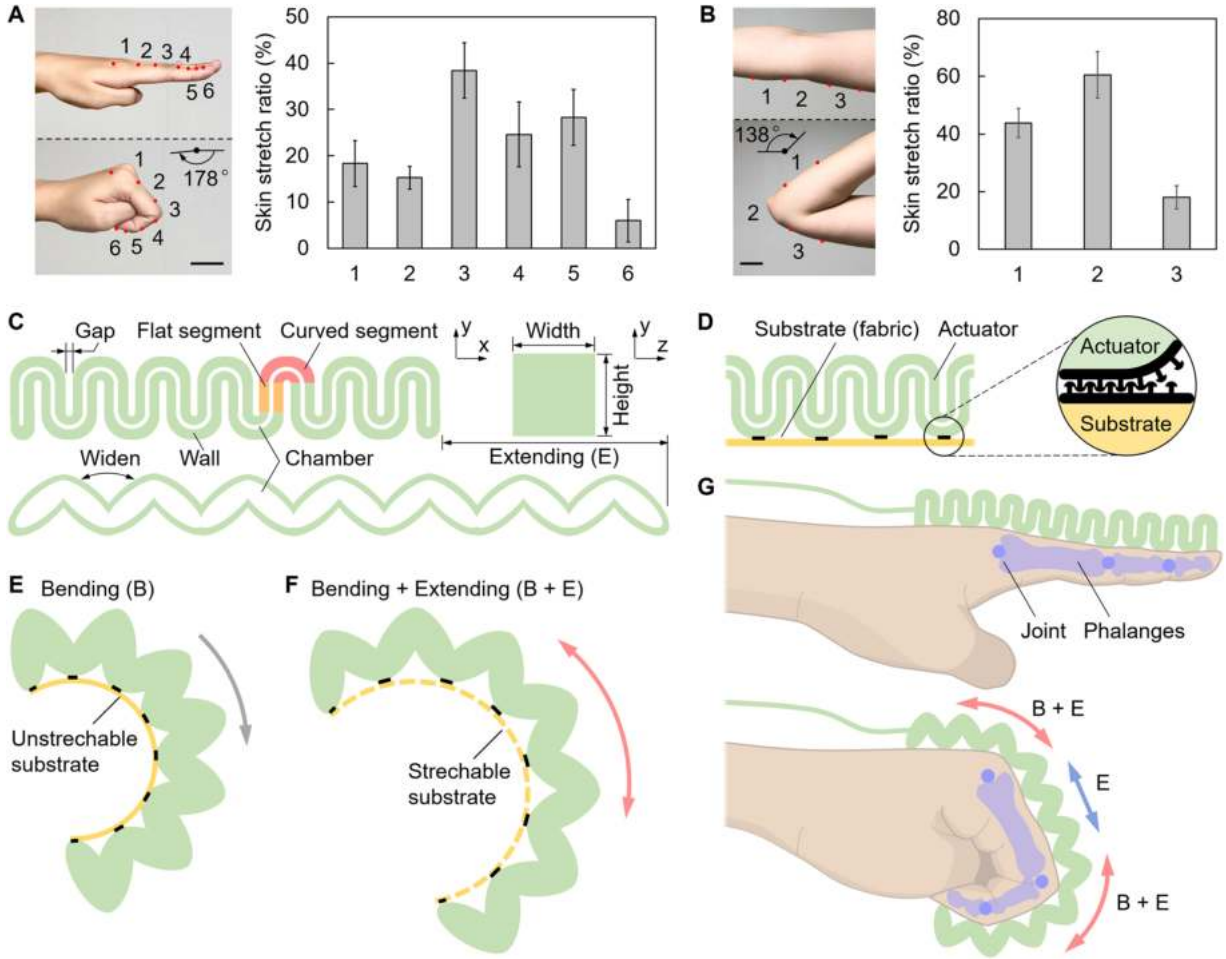

Fig. 1. Design and working principle of DPSA with adaptive deformation. (A,B) The skin stretch ratio caused by flexion of the forefinger (A) or the elbow (B) with a sample size of five individuals. When the finger flexes (about 178°) or the elbow rotates (about 138°), the incremental distance between every two adjacent marks along the outer contour of the finger or elbow as the amount of stretching of the skin between the two marks. Scale bars are 30 mm. (C) The cross-sectional view shows the soft linear actuator before (top) and after (bottom) pressurization. (D) The RFs on each segment enable the DPSA to be easily fixed on the substrate. (E) The nonstretchable substrate enables the DPSA to generate pure bending deformation. (F) The stretchable substrate enables the DPSA to generate the bending-extending coupled deformation. (G) Concept application for wearables (fasteners and fabric gloves are not indicated).

bonding fasteners as the temporary bond to form the DPSA, which inherits the linear actuator's softness and compliance while being easily attached to many substrates (Fig. 1D).

The temporary bonding fasteners used in this study are reclosable fasteners (RFs, Dual Lock, 3 M), and other temporary bonds such as hook-and-loop fasteners also work. Once attached to a substrate, the DPSA under pressurization can produce bending deformation to the side with RFs and adapt well to the stretch of the substrate. That is, an unstretchable substrate enables the DPSA to produce pure bending deformation, and a stretchable substrate enables the DPSA to produce bending and extending coupled deformation (Fig. 1E and F). Furthermore, the discrete RFs enable the DPSA to easily conform to various shapes and surfaces. These characteristics of the DPSA cater to the needs of wearable devices for motion assistance. As one example of wearable gloves, DPSA can adapt well to the stretch of the finger skin when bending a finger, that is, DPSA can adaptively bend and extend at finger joints but only extend at phalanges (Fig. 1G).

To design a compact DPSA, the projection of the DPSA in the length direction is designed in a squared shape with both height and width determined as 10 mm. The gap between the neighbor segments, wall thickness, and chamber thickness are all determined as 1 mm (Fig. 1C). Fig. 2 shows the main fabrication process of the DPSA. First, the outer mold and an inner core made of acrylonitrile butadiene styrene (ABS) were fabricated via 3D printing. The inner core was designed with the same shape as the air chamber. Then, the inner core was positioned on the mold through the locating points, the mold was filled with liquid polymer (Dragon Skin 30, Smooth-on), the assembly was covered with cover mold, and the assembly was cured at 60 ℃ for 4 h. Afterward, the cured assembly was immersed in acetone to dissolve the mold, cover, and inner core (Fig. 2A). After that, the holds on the actuator that let the acetone flow in and out were patched up with liquid polymer and cured again. Finally, the RFs were bonded using adhesive (Sil-Poxy, Smooth-On), and a tube was attached to the actuator (Fig. 2B).

3. Results and discussion

3.1. Extending deformation of DPSA

The first experiment was conducted to evaluate the effect of the pressures applied to the linear extension rate of the DPSAs. The actuator with a length of 140 mm was hung vertically by fixing its one end and actuated using pressures ranging from 0 kPa to 90 kPa in increments of 10 kPa. The results are shown in Fig. 3A for the extension rate of the DPSA at different applied pressures. The results show that the extension rate goes up along with an increase in the applied pressure, and the

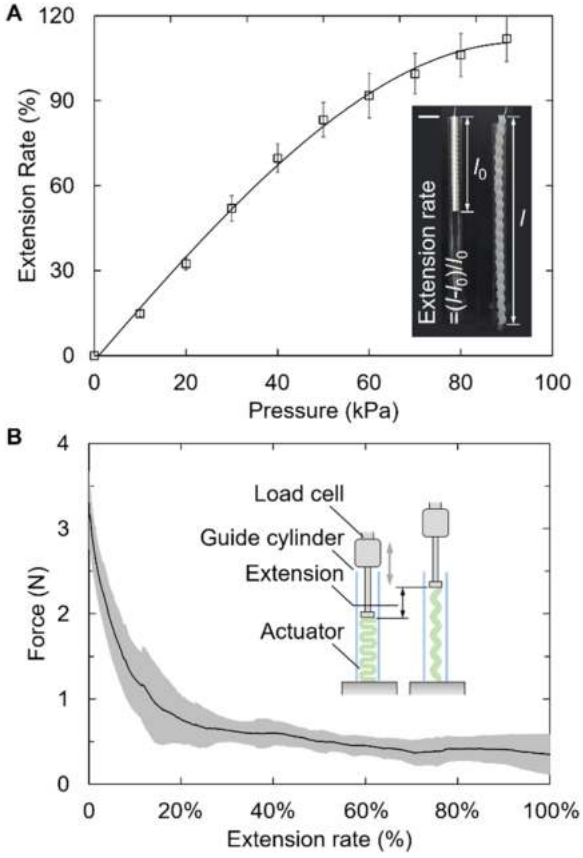

Fig. 3. Performance evaluations of the extending deformation. (A) The elongation of the DPSA (without substrate). The variable l_0 is the length of the vertically hung actuator at 0 kPa, and l is the length of the extended actuator under pressurization. The inset shows the elongation of the DPSA at 90 kPa. (B) The linear blocking force of the DPSA (without substrate) at different extension rates. The inset shows the experimental setup. Scale bar: 30 mm.

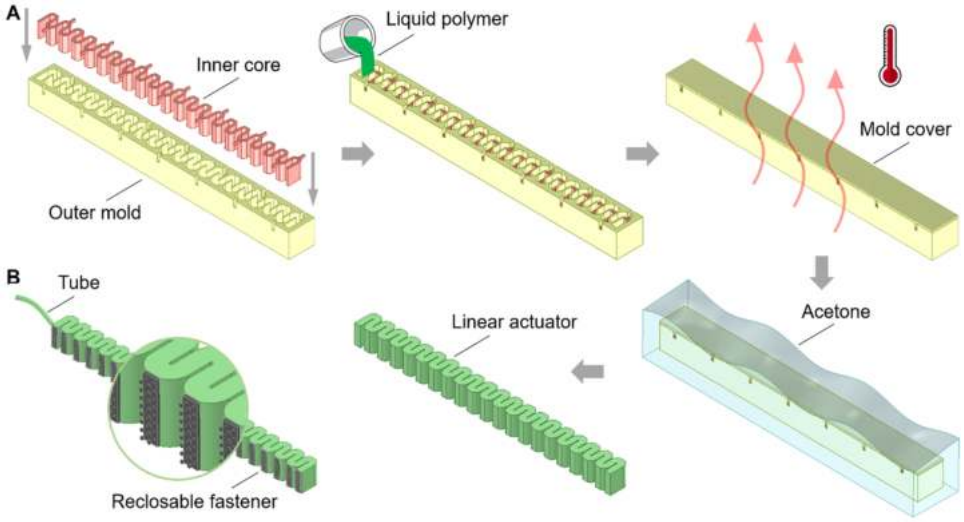

Fig. 2. Fabrication process of the DPSA. (A) Fabrication of the soft linear actuator. The outer mold and the inner core are assembled, the liquid polymer is poured, the liquid elastomer is thermally cured, and then the assembly is fully soaked in acetone to melt both the inner and outer molds thoroughly to obtain the soft linear actuator. (B) The RFs were bonded to each segment on one side of the linear actuator and a tube was attached to the actuator.

increase rate gradually slows down. The results also show that the applied pressure of 90 kPa results in a corresponding extension rate of 112 %, that is, more than double its original length.

The following experiment was conducted to measure the extension force of the DPSA. The actuator with the fixed bottom end was placed vertically inside a cylindrical tube to guide the actuator to extend straight upward. The other end of the DPSA before pressurization is directly against a solid bar rigidly fixed to a load cell (SMT1–5 N, Interface) with positions controlled by a universal tensile tester (AGS-X Series, Shimadzu). The DPSA was first pressurized at a constant pressure of 90 kPa, and then the load cell slowly moved upward at 3 mm/s, which is slow, in order to ensure that the actuator can be fully inflated at any instantaneous position. The force measured by the load cell is recorded in Fig. 3B, and the results show that the extension force starting at 3.3 N without extension significantly decreases as the load cell goes upward until 0.78 N at an extension rate of around 20 % and then slightly decreased afterward until 0.34 N at 100 %.

3.2. Bending–extending coupled deformation of DPSA

A key feature of the DPSA is that it can adapt to stretchable substrates. A method is demonstrated to measure the deformation of the

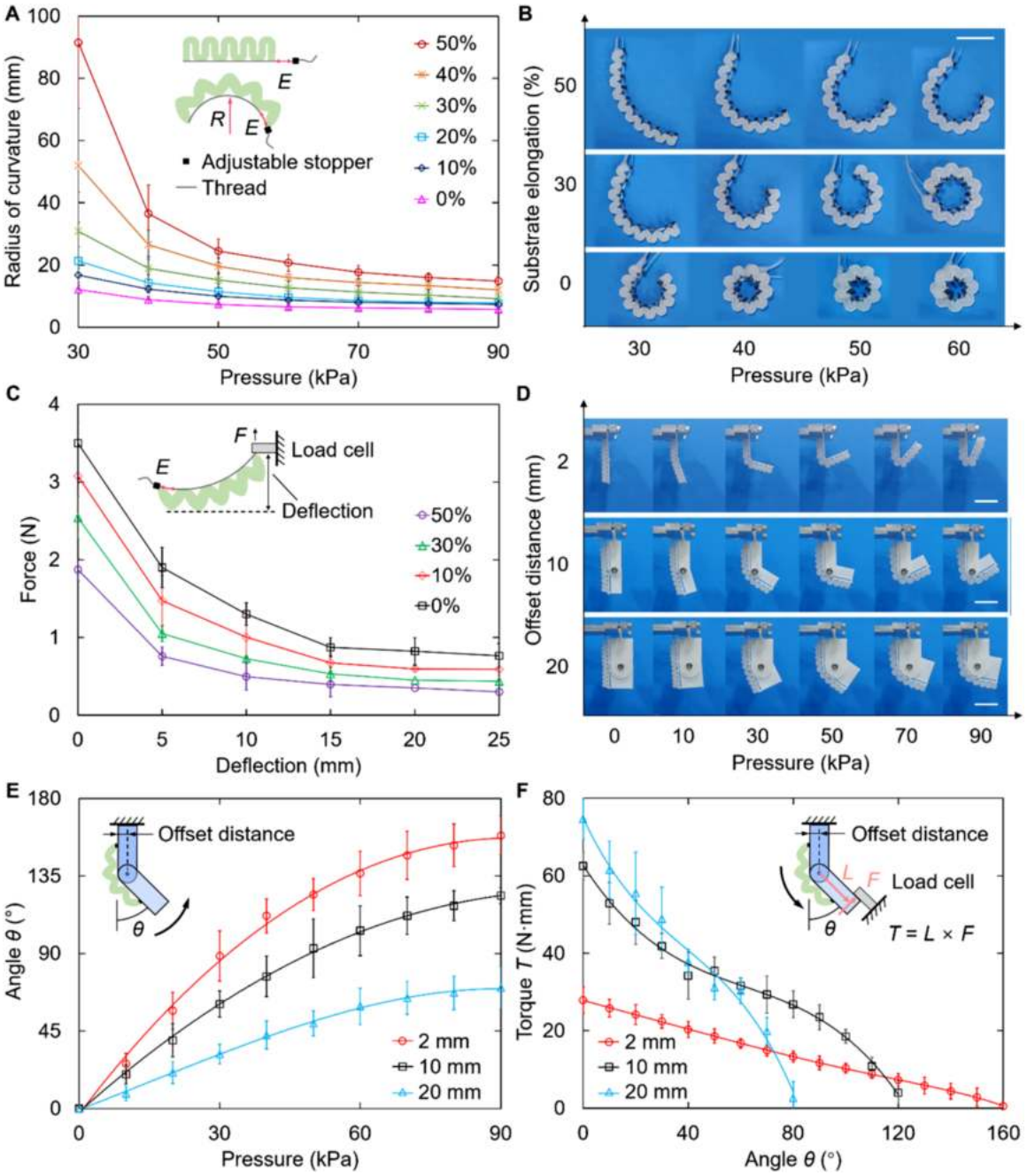

Fig. 4. Performance evaluations of the bending–extending coupled deformation. (A) The radius of the curvature of the bending deformation of the DPSA with different substrate elongations at various applied pressures. The inset shows the experimental setup. (B) Photographs of the deformation of DPSA with a substrate elongation of 0 %, 30 %, and 50 % at 30, 40, 50, and 60 kPa, respectively. (C) Blocking forces of the DPSA with a substrate elongation ranging from 0 % to 50 % in increments of 10 % at 90 kPa. (D) Photographs of the deformation of the hinges with attached DPSA at an offset distance of 2 mm, 10 mm, and 20 mm at various applied pressures. (E) Bending angle of the hinge under various offset distances of DPSA at various applied pressures. (F) Torque-angle relationship of the hinge under various offset distances. All scale bars are 30 mm.

DPSA to different stretchable ratios of the substrates, and the schematic of the experimental setup is shown in the inset in Fig. 4A. A rigid fixer with a small hole is attached to each fastener of the DPSA, and they were threaded with a nylon string along the longitudinal direction of the DPSA. Extension of the DPSA is limited ranging from 0 % to 50 % in increments of 10 % by manually adjusting the location of the stopper at the end of the string. During the test, the DPSA initially extended straight as pressure increased and then started to bend after reaching the stopper. The experiments were conducted on a horizontal flat surface to exclude the effect of gravitational force. Results show that the DPSA can adapt to substrates with different stretchable ratios to obtain the corresponding deformation (Fig. 4B). Results also show that a larger extension ratio will result in a larger radius of bending curvature at a specified pressure, and a larger pressure will result in a smaller radius of bending curvature at a specified extension ratio (Fig. 4A).

The blocking forces of the DPSA were also measured. The experiment was conducted for tip deflections of DPSA, at 90 kPa, varying from 0 mm to 25 mm by adjusting the height of the load cell in increments of 5 mm. One end of the DSPA is fixed and the whole actuator is placed on a smooth plate to neglect the effect of the friction on the extending deformation of the DSPA. The schematic of the experimental setup is shown in the inset of Fig. 4C. When inflating the DSPA, the force generated by the free end along the vertical direction is measured and plotted in Fig. 4 C. The results show that a larger extension leads to a smaller blocking force, and the blocking force decreases rapidly as the deflection increases.

One application for accommodating stretchable substrates in wearables is that the soft actuators can be attached to body joints at different offset distances. This capability of the DPSA was evaluated by attaching an actuator with a length of 70 mm to rigid hinges with different offset distances (i.e., vertical distances from the joint center to the surface where the DPSA is attached) as 2 mm, 10 mm, and 20 mm. The rigid hinge consists of two links, and a joint is hung vertically by fixing the upper link. Both ends of the DPSA were fixed to the two links via RFs, respectively, and the actuator together with the links was winded by a nylon line to prevent it from being distorted sideways. The bending deformation of the rigid hinges at different applied pressure is described in Fig. 4D. Results show that the amount of the maximum bending

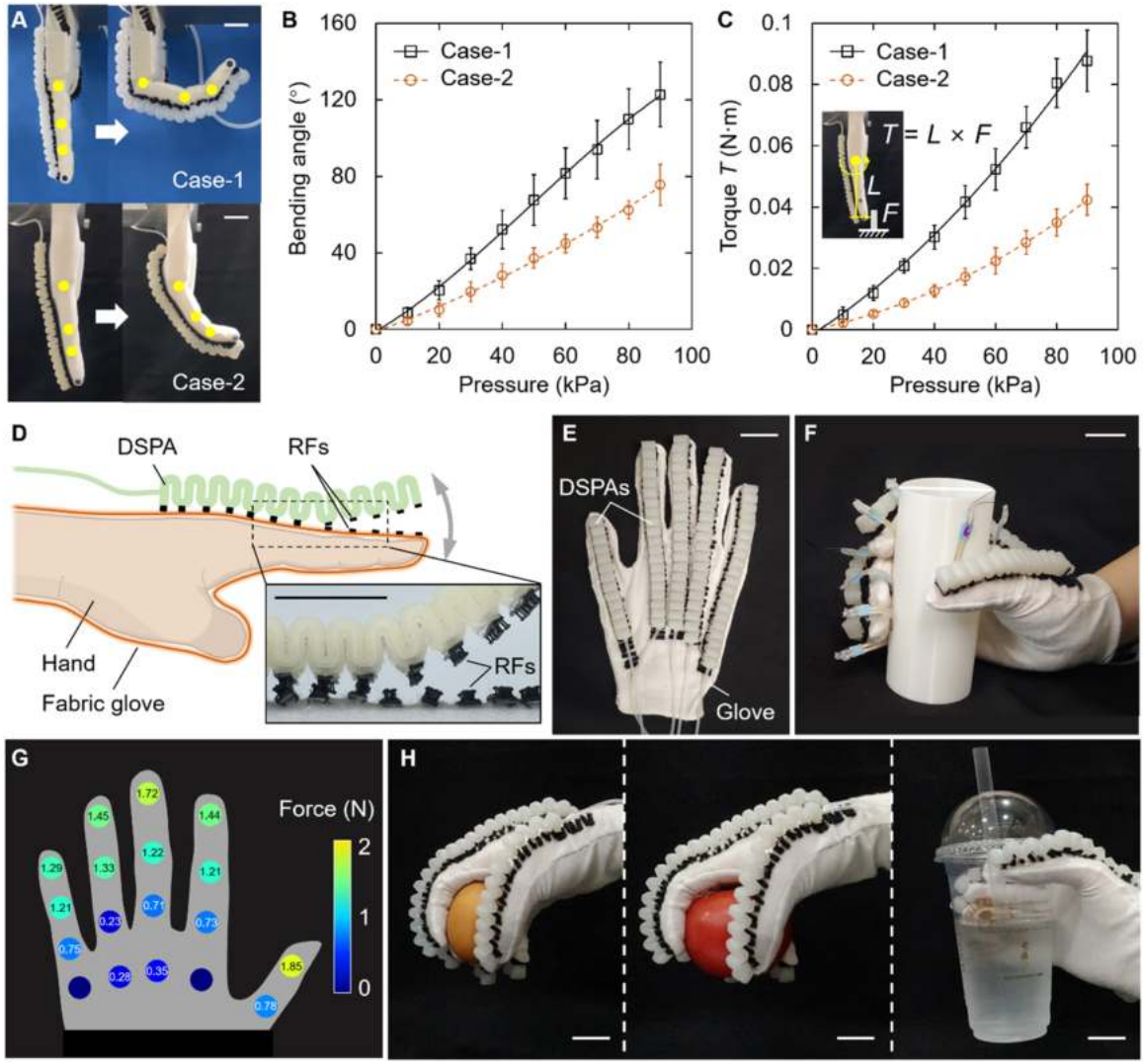

Fig. 5. Design and performance evaluation of the soft robotic glove. (A) The DSPA with uniformly distributed RF segments (case-1) and the DSPA with a monolithic RF sheet (case-2) enables a hinged finger to achieve a maximum bending deformation of about 122.8° and 90.8° at 90 kPa, respectively. (B) The bending angle of the finger changes as the applied air pressure increases in both cases. (C) Torque measurement related to the topmost joint of the finger at different applied pressures. (D) Schematic of DPSAs easily bonding to or separating from the desired fabrics worn by the body parts for reuse and exchange. The inset shows the corresponding operation. (E) Fabric glove with bonded DPSA on each finger. (F) Grasping hollow cylinder with a diameter of 50 mm using the DPSA glove installed with force sensors. (G) Pressure map of grasping the cylinder. (H) Grasping an egg, a tomato, and a bottle half filled with water by wearing the glove. All scale bars are 20 mm.

deformation is inversely proportional to the magnitude of the offset distances, where the bending angles are 158.5°, 123.7°, and 70.1° at 90 kPa for an offset distance of 2 mm, 10 mm, and 20 mm, respectively (Fig. 4E). The torque of the hinge at the different bending angles at 90 kPa was also measured by placing the same load cell each time perpendicular to the link that can rotate. The torque was calculated by multiplying the distance between the joint center and the load cell, and the amount of force was measured by the load cell. The results show that the torque decreases as the bending angle increases, and the maximum torques obtained at the initial position were 74.7 N·mm, 62.6 N·mm, and 27.9 N·mm for an offset distance of 2 mm, 10 mm, and 20 mm, respectively (Fig. 4F).

3.3. Application to a soft robotic glove

The proposed DPSA allows for attaching to the dorsal side of the joints of the human body through stretchable fabrics, such as finger and elbow joints, and accommodating to body movements via adaptive bending and extending deformation. The fabrics are sewn with many evenly distributed small pieces of RF. When wearing these fabrics, DSPAs can be directly bonded to the fabric covering the skin through its RFs or can be separated from the fabric through shearing force. A single DSPA with evenly distributed RF segments (case-1) was attached to a finger structure with three joints mimicking a human finger (Fig. 5A). Upon pressurization at 90 kPa, the DSPA enables the finger structure to reach a bending deformation of about 122.8°. As a comparison, a DSPA with a monolithic non-stretchable RF sheet (case-2) was attached to the same finger structure, which results in a bending deformation of about 90.8°, that is, the deformation is lost by 26.1 % (Fig. 5B). The torque of the finger structure at a zero bending angle was also measured using a similar experimental setup for the torque test of the DPSA. The results show the torque generated by the finger increases as the applied air pressure increases (Fig. 5C). Moreover, the torques generated by the DSPA of case-1 and case-2 are around 0.09 N·m and 0.04 N·m, that is, the torque produced by case-1 is 2.25 times that of case-2. Overall, when attached to joints, the DSPA with evenly distributed RFs can produce significantly more bending deformations and torques than the one with a monolithic non-stretchable RF sheet.

Five DPSAs were then applied to the design of a soft robotic glove where a DPSA is fixed on each finger of the glove by RFs. The glove is made of moderately stretchy fabric, and the RF is cut into small pieces and sewn evenly on the dorsal side of the glove's fingers (Fig. 5D and E). The DPSAs can easily bond to or separate from the desired fabrics for reuse and exchange. To measure the magnitude of the force from the glove applied to static objects, a hollow cylinder with a diameter of 50 mm was selected as the target object to simulate grasping the actual object because a hand can easily hold more than half the circumference of the cylinder (Fig. 5F). A total of eighteen force sensors (DF9–40, Leanstar) were attached to the ventral side of the glove, and these sensors were located at the phalanges and the upper part of the palm that come into contact with the grasped objects. Fig. 5G depicts the corresponding pressure map at 90 kPa for grasping the cylinder with the only force generated by the DPSAs. Most pressures ranging between 1.3 N and 1.8 N were located in the front part of the fingers, which is also the part that mainly comes into contact with the grasped object. To enhance the friction between the glove and objects, a thin layer of elastomer membrane (Ecoflex 35, Smooth-on) was attached to the tip of the glove fingers. The grasping performance was also evaluated by wearing the glove to grab different objects, including a raw egg (60 g), a tomato (150 g), and a cup of water (250 g) (Fig. 5H).

3.4. Application to elbow assistance

To further demonstrate the performance of the DPSA, parallelized DPSAs for high-force generation were used to bend an elbow-like mechanism with a larger offset distance. An elbow-like mechanism with the real scale was fabricated and put on an elastic armband with sewed RFs. Instead of sewing a whole piece of RF onto the armband, the RFs were distributed evenly and discretely on the band in pixelated small pieces. Then, a total of eight DPSAs in parallel in the longitudinal direction were attached to the armband (Fig. 6A). Under pressurization, the eight parallelized DPSAs enable the arm to bend around 90° at 90 kPa (case-1) (Fig. 6B). As a comparison, the eight parallelized DPSAs were then attached to the elbow joint through a monolithic RF sheet (case-2), which results in a very small bending deformation of about 2.5° (Fig. 6C). Fig. 6D further shows the bending angle of the arm to the applied pressure for both cases. The results show that as the applied pressure increases, the bending angle of the robotic arm for case-1 also increases, and it can be approximated as no bending deformation occurs for case-2. Compared with the small deformation of the finger structure, the arm hardly has any bending deformation, because a much larger offset distance results in these soft bending actuators containing non-stretchable constraining layers that buckle and cannot bend due to high inconsistency between the stretch of soft actuators and that required by the skin.

The torque of the robotic elbow at a zero bending angle was also tested using a similar experimental setup for the torque test of the DPSA. The results show there is a positive correlation between the applied pressures and the generated torque, and the maximum torque for case-1 at 90 kPa was about 0.41 N·m (Fig. 6E). However, it is worth noting that the total torque was less than the value of the number of DPSAs multiplied by the torque of one actuator. That is because, due to the round cross-section of the mannequin arm, the DPSAs placed on the side cannot directly deliver all their forces to bend the arm. That is, the force generated by the actuators on the side is not in the plane of motion of the robotic elbow, so only their vertical force components contribute to the bending deformation, as shown in the inset in Fig. 6B.

4. Conclusions

In summary, this study demonstrated a DPSA with the purpose of improving a soft actuator's adaptability, conformality, and usability for wearable applications. The DPSA was formed by bonding RFs uniformly distributed to one side of a soft linear actuator. The RFs enable the DPSAs to be easily attached to the fabrics to provide a conformal fit to the user's body part. The fabrics attached with DPSAs, through evenly distributed RF segments instead of a single piece of RF, are capable of not only actively deforming to flex the body joints efficiently but also passively adapting to the stretching deformation of the skin caused by joint motion. Accordingly, the DPSA is not constrained by the offset distance between the joint and the DPSA. The user can apply it for a broadened application range. Moreover, the high-force requirement can be satisfied by using parallelized DPSAs. In addition, DPSAs in a single design supported by temporary bonding fasteners are capable of good interchangeability and replaceability to reduce the complex design process and save fabrication costs. As demonstrations, wearable fabrics with DPSAs were designed for both the soft robotic glove and elbow assistance. Although the great differences in the joint dimensions of the finger and elbow resulted in obvious offset distances, the DPSAs bent them successfully, even when a single design was used. Future work will focus on optimizing the structural design of DPSAs and improving their pressure resistance to output a stronger actuating force for even more practical applications.

Declaration of Competing Interest

The authors declare that they have no known competing financial interests or personal relationships that could have appeared to influence the work reported in this paper.

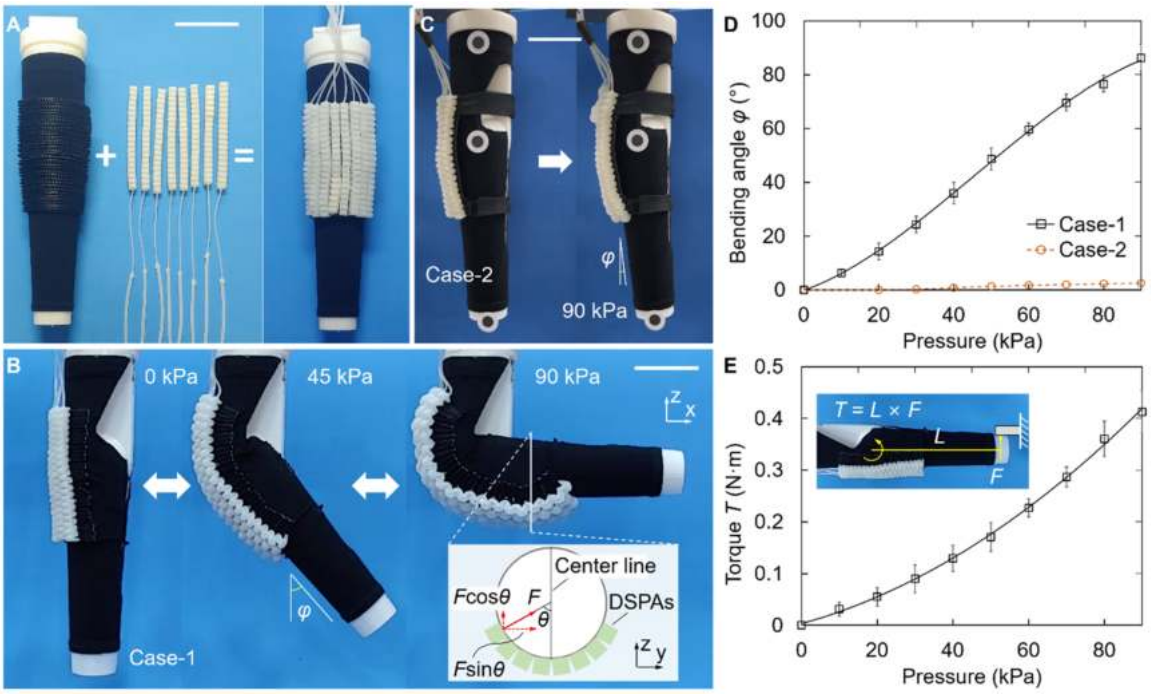

Fig. 6. Design and performance evaluation of the robotic elbow. (A) Eight DPSAs were attached to the elbow joint via fabrics using evenly distributed pixelated small pieces of RFs (case-1). (B) Bending deformation of the robotic elbow under pressurization. The inset shows the schematics of the cross-section of the robotic arm with attached DPSAs and the resolution of the bending force of a DPSA placed on the side. (C) Eight DSPAs are attached to the elbow joint using a monolithic RF sheet (case-2). (D) The maximum bending angle of the elbow joint attached with DPSAs, for case-1 and case-2, at different applied pressures. (E) Torque measurement of the robotic elbow attached with DPSAs of case-1 at different applied pressures. All scale bars are 70 mm.

Data Availability

Data will be made available on request.

Acknowledgments

This work was supported by the National Research Foundation of Korea (NRF) grant funded by the Ministry of Science and ICT (MSIT), Korea government (No. 2020R1C1C1010295). The authors would like to give the most thanks to the Lord Jesus Christ.

References

[1] K. Kong, D. Jeon, Design and control of an exoskeleton for the elderly and patients, IEEE/ASME Trans. Mechatron. 11 (2006) 428–432, https://doi.org/10.1109/TMECH.2006.878550.
[2] A.H. Börsch-Supan, The impact of global aging on labor, product, and capital markets, Popul. Dev. Rev. 34 (2008) 52–77.
[3] B.H. Dobkin, Strategies for stroke rehabilitation, Lancet Neurol. 3 (2004) 528–536, https://doi.org/10.1016/S1474-4422(04)00851-8.
[4] P. Langhorne, J. Bernhardt, G. Kwakkel, Stroke rehabilitation, Lancet 377 (2011) 1693–1702, https://doi.org/10.1016/S0140-6736(11)60325-5.
[5] C. Thalman, P. Artemiadis, A review of soft wearable robots that provide active assistance: trends, common actuation methods, fabrication, and applications, Wearable Technol. 1 (2020) 1–27, https://doi.org/10.1017/wtc.2020.4.
[6] F. Iida, C. Laschi, Soft robotics: challenges and perspectives, Procedia Comput. Sci. 7 (2011) 99–102, https://doi.org/10.1016/j.procs.2011.12.030.
[7] C. Laschi, B. Mazzolai, M. Cianchetti, Soft robotics: Technologies and systems pushing the boundaries of robot abilities, Sci. Robot 3690 (2016) eaah3690, https://doi.org/10.1126/scirobotics.aah3690.
[8] M. Calisti, G. Picardi, C. Laschi, Fundamentals of soft robot locomotion, J. R. Soc. Interface (2017) 14.
[9] W.D. Wang, Z. Ding, Y. Lee, X. Han, Engineering liquid-vapor phase transition for refreshable haptic interfaces, Research (2022), 9839815.
[10] A. Dwivedi, L. Gerez, W. Hasan, C.H. Yang, M. Liarokapis, A soft exoglove equipped with a wearable muscle-machine interface based on forcemyography and electromyography, IEEE Robot Autom. Lett. 4 (2019) 3240–3246, https://doi.org/10.1109/LRA.2019.2925302.
[11] L. Gerez, J. Chen, M. Liarokapis, On the development of adaptive, tendon-driven, wearable exo-gloves for grasping capabilities enhancement, IEEE Robot Autom. Lett. 4 (2019) 422–429, https://doi.org/10.1109/LRA.2019.2890853Y.
[12] B.B. Kang, H. Choi, H. Lee, K.J. Cho, Exo-glove poly II: a polymer-based soft wearable robot for the hand with a tendon-driven actuation system, Soft Robot 6 (2019) 214–227, https://doi.org/10.1089/soro.2018.0006.
[13] M. Manti, T. Hassan, G. Passetti, N. D'Elia, C. Laschi, M. Cianchetti, A bioinspired soft robotic gripper for adaptable and effective grasping, Soft Robot 2 (2015) 107–116, https://doi.org/10.1089/soro.2015.0009.
[14] M. Xiloyannis, L. Cappello, D.B. Khanh, S.C. Yen, L. Masia, Modelling and design of a synergy-based actuator for a tendon-driven soft robotic glove, Proc. IEEE RAS EMBS Int Conf. Biomed. Robot Biomechatronics (July) (2016) 1213–1219, https://doi.org/10.1109/BIOROB.2016.7523796.
[15] S.J. Park, C.H. Park, Suit-type wearable robot powered by shape-memory-alloy-based fabric muscle, Sci. Rep. 9 (2019) 1–8, https://doi.org/10.1038/s41598-019-45722-x.
[16] J. Jeong, I.Bin Yasir, J. Han, C.H. Park, S.K. Bok, K.U. Kyung, Design of shape memory alloy-based soft wearable robot for assistingwrist motion, Appl. Sci. (2019) 9, https://doi.org/10.3390/app9194025.
[17] J. Jeong, K. Hyeon, J. Han, C.H. Park, S.Y. Ahn, S.K. Bok, et al., Wrist assisting soft wearable robot with stretchable coolant vessel integrated SMA muscle, IEEE/ASME Trans. Mechatron. (2021), https://doi.org/10.1109/TMECH.2021.3078472.
[18] W. Wang, Y. Tang, C. Li, Controlling bending deformation of a shape memory alloy-based soft planar gripper to grip deformable objects, Int. J. Mech. Sci. 193 (2021), 106181, https://doi.org/10.1016/j.ijmecsci.2020.106181.
[19] P.H. Nguyen, W. Zhang, Design and computational modeling of fabric soft pneumatic actuators for wearable assistive devices, Sci. Rep. 10 (2020) 1–13, https://doi.org/10.1038/s41598-020-65003-2.
[20] J.W. Booth, D. Shah, J.C. Case, E.L. White, M.C. Yuen, O. Cyr-Choiniere, et al., OmniSkins: robotic skins that turn inanimate objects into multifunctional robots, Sci. Robot 3 (2018) 1–10, https://doi.org/10.1126/scirobotics.aat1853.
[21] Q. Zhao, Y. Wang, H. Cui, X. Du, Bio-inspired sensing and actuating materials, J. Mater. Chem. C 7 (2019) 6493–6511, https://doi.org/10.1039/c9tc01483g.
[22] C. Tawk, Y. Gao, R. Mutlu, G. Alici, Fully 3D printed monolithic soft gripper with high conformal grasping capability, IEEE/ASME Int Conf. Adv. Intell. Mechatron., AIM (July) (2019) 1139–1144, https://doi.org/10.1109/AIM.2019.8868668.
[23] B.W.K. Ang, C.H. Yeow, Print-it-Yourself (PIY) glove: a fully 3D printed soft robotic hand rehabilitative and assistive exoskeleton for stroke patients, IEEE Int Conf. Intell. Robot Syst. (September) (2017) 1219–1223, https://doi.org/10.1109/IROS.2017.8202295.
[24] F. Connolly, C.J. Walsh, K. Bertoldi, Automatic design of fiber-reinforced soft actuators for trajectory matching, Proc. Natl. Acad. Sci. 114 (2017) 51–56, https://doi.org/10.1073/pnas.1615140114.
[25] K.C. Galloway, K.P. Becker, B. Phillips, J. Kirby, S. Licht, D. Tchernov, et al., Soft robotic grippers for biological sampling on deep reefs, soro.2015.0019, Soft Robot (2016) 3, https://doi.org/10.1089/soro.2015.0019.

[26] R.V. Martinez, C.R. Fish, X. Chen, G.M. Whitesides, Elastomeric origami: programmable paper-elastomer composites as pneumatic actuators, Adv. Funct. Mater. 22 (2012) 1376–1384, https://doi.org/10.1002/adfm.201102978.
[27] P. Polygerinos, S. Lyne, Z. Wang, L.F. Nicolini, B. Mosadegh, G.M. Whitesides, et al., Towards a soft pneumatic glove for hand rehabilitation, IEEE Int Conf. Intell. Robot Syst. (2013) 1512–1517, https://doi.org/10.1109/IROS.2013.6696549.
[28] Z. Wang, P. Polygerinos, J.T.B. Overvelde, K.C. Galloway, K. Bertoldi, C.J. Walsh, Interaction forces of soft fiber reinforced bending actuators, IEEE/ASME Trans. Mechatron. 22 (2017) 717–727, https://doi.org/10.1109/TMECH.2016.2638468.
[29] K.H.L. Heung, R.K.Y. Tong, A.T.H. Lau, Z. Li, Robotic glove with soft-elastic composite actuators for assisting activities of daily living, Soft Robot 6 (2019) 289–304, https://doi.org/10.1089/soro.2017.0125.
[30] H.K. Yap, J.H. Lim, F. Nasrallah, J.C.H. Goh, R.C.H. Yeow, A soft exoskeleton for hand assistive and rehabilitation application using pneumatic actuators with variable stiffness, Proc. - IEEE Int Conf. Robot Autom. (2015-June) (2015) 4967–4972, https://doi.org/10.1109/ICRA.2015.7139889.
[31] J. Wang, Y. Fei, W. Pang, Design, modeling, and testing of a soft pneumatic glove with segmented pneunets bending actuators, IEEE/ASME Trans. Mechatron. 24 (2019) 990–1001, https://doi.org/10.1109/TMECH.2019.2911992.
[32] H. Yang, S. Jin, W.D. Wang, Modular assembly of soft machines via multidirectional reclosable fasteners, Adv. Intell. Syst. (2022), 2200048, https://doi.org/10.1002/aisy.202200048.

Haewon Jeong received the B.S. degree from the Department of Mechanical Engineering, Hanyang University, Korea, in 2021. She is currently a M.S. candidate in Mechanical Engineering at Hanyang University, Korea, and her research interests include soft robotics and bioinspired robotics.

Wei Dawid Wang received the B.S. and M.S. degrees from the School of Mechatronics Engineering, Harbin Institute of Technology, China, in 2008 and in 2011, and the Ph.D. degree from the Department of Mechanical Engineering, Seoul National University, Korea, in 2016. He is currently an Assistant Professor of Mechanical Engineering at Hanyang University. His research interests include soft robotics, bioinspired robotics, and smart materials & structures.